

Quantitative Assessment of Reheated Coconut Oil Using Transmittance Multi Spectral Imaging

S.Keerthana¹, K.Sathishkumar², K.sedhu³, N.Soundirarajan⁴, R.Vignesh⁵

Department of Electronics and Communication Engineering, V.S.B. Engineering College, Karur, India.

Abstract— This paper focuses on oil reheating analysis using multispectral images. The quality of food consumed has a considerable influence on the health of a society. A machine learning method and a multispectral image are used to forecast the reheating of oil state. Then, a new strategy for creating a spectral-clustering based classifier to determine the impact of warming and reusing coconut oil is provided. Varied clusters were discovered for different quantities of reheated oil classes on training samples, and classification was accomplished with an accuracy of 0.983. In addition, the input images for the recommended algorithms are made with an in-house application.

Keywords— Oil Reheating, Multispectral Picture, Oil Condition, Input Photos

I. INTRODUCTION

Coconut (*Cocos nucifera*) is a versatile palm tree with multiple applications. The fibrous one-seeded drupe is used to make coconut water, coconut milk, dried coconut, and coconut oil. Coconut oil has been used in a variety of ways, including as a cooking or frying oil, as a component in a range of foods, in the creation of skincare products, and in the manufacture of pharmaceuticals. Due to its reduced manufacturing cost, palm oil, which has similar physical properties to coconut oil, is widely used to adulterate coconut oil [1]. Furthermore, foodservice establishments and families routinely reuse frying oil to save money. As a result, the chemical and thermophysical properties of edible oils are changed during reuse, jeopardizing their safety and rendering fried foods unfit for consumption. A multispectral imaging system was created using nine spectral bands with peak wavelengths ranging from 405 nm to 950 nm. A method was created using Principal Component Analysis (PCA) and Bhattacharyya Distance.

This paper is further arranged as follows. Section II gives the multispectral imaging spectrum. Section III explains about the deep learning. Section IV explain the related works. Section V represents the proposed methodology. Experimental results are given in Section VI and Section VII concludes the paper.

II. MULTISPECTRAL IMAGING SPECTRUM

The bulk of multispectral imaging research reported in the literature rely on the reflective properties of opaque materials. This strategy, however, is only loosely relevant to most liquids since only a tiny proportion of light is reflected. To examine the transmittance spectrum of liquids, a low-cost multispectral imaging device was developed [2]. This imaging system can capture monochrome multispectral images from ultraviolet (UV) to near-infrared (NIR) with an overall resolution of 9 spectral bands (NIR). The LEDs that were used in this project are thoroughly detailed. The imaging system used in this work has a number of key components. A 10-bit CMOS monochrome camera (FLIR Blackfly S Mono, 1.3 MP, USB3 Vision camera, Resolution – 1280x1024) was put on top of the portable dark chamber to capture the transmittance spectrum of a sample.

This camera can capture images in the 350 to 1080 nanometer spectral range. A laptop was used to capture the image and send commands to both the discovery board (STM32F0DISCOVERY) and the monochrome camera (MSI GE626QD). In the portable dark room, an LED switching circuit made up of nine off-the-shelf LEDs was fitted. An integrating hemisphere made of aluminum with a 130mm inner diameter was used to offer better illumination for the sample. A locally manufactured AC regulated 12V DC power supply unit was used to give stable power input to the LED driver ICs (MAX16839ASA+). In front of the LED switching circuit, the camera was positioned.

The camera was calibrated properly to generate a well-focused image, and the aperture was adjusted to avoid saturated pixels in the image. Two USB connections were used to link the camera and the discovery board to the laptop computer. In a cylindrical container, the liquid sample was kept. PVC tubing was used for the container's walls, while 2 mm plain glass was used for the base.

III. DEEP LEARNING

Deep learning, sometimes called deep structured learning or hierarchical learning, which is a type of machine learning that learns from data rather than task-specific algorithms. The three types of learning are unsupervised, semi-supervised, and supervised. In recent years, academics have been particularly interested in employing

image processing as well as computer vision techniques that detect fire in photos. If they are accurate enough, such systems may even surpass ordinary fire detection technologies.

One of the most promising techniques in this sector is convolutional neural networks (CNNs). Previous fire detection research employing CNNs, on the other hand, has only focused on balanced datasets, which might give erroneous information about real-world performance in locations where fire is infrequent. In fact, as this study shows, a typical CNN performs poorly when evaluated on the more realistically balanced benchmark dataset provided in this study. As a result, for image fire detection, we recommend utilizing even deeper Convolutional Neural Networks, with fine tuning based on a fully connected layer. VGG16 and Resnet50, two pre-trained state-of-the-art Deep CNNs, are used in our fire detection system. On an imbalanced dataset that we built to imitate real-world situations, the Deep CNNs are put to the test. It includes shots that are extremely difficult to describe, as well as images that are purposely unbalanced, with many more non-fire images than fire images.

Adding completely connected layers for fine tuning enhances accuracy while dramatically increasing training time, according to our findings. It may be used to train artificial intelligence to anticipate outcomes consist of a collection of inputs. To train the AI, both supervised and unsupervised learning methodologies can be applied. We'll investigate deep learning by building a fictitious airline ticket price estimator service. Because models may adjust autonomously as they are exposed to fresh data, the iterative feature of machine learning is critical. Convolutional neural networks (CNNs, or ConvNets) a type of deep neural network used to analyze images. Individual cortical neurons that only respond to stimuli that fall inside the receptive field, which is a small portion of the visual field.

IV. RELATED WORKS

A strategy for distinguishing and quantifying refined, bleached, and deodorized (RBD) pure coconut oil (PCO) from 26 its adulterant RBD fried coconut oil was devised using attenuated total reflection-Fourier transform infrared (ATR-FTIR) spectroscopy and 24 multivariate regression modeling (FCO). This study [1] will aid the oil industry and regulatory agencies since it gives essential information 37 for building standard methodologies for detecting oil adulteration.

A multispectral imaging method for determining the proportion of tartrazine colored rice flour in turmeric powder, a typical adulterant. Nine spectral bands having peak wavelengths ranging between 405 nm to 950 nm were used to develop a multispectral imaging system. Principal Component Analysis (PCA) and Bhattacharyya Distance

were used to develop a technique. A second-order polynomial was used to model the link between the Bhattacharyya Distance and the extent of adulteration. [2]

To measure smoke point, oxidative stability, free fatty acids, polar compounds, fatty acid profiles, and UV coefficients, extra virgin olive oil (EVOO) and other common cooking oils were heated to 240°F and then subjected to 180°F for 6 hours, with samples collected at different intervals. In contrast to oils like canola oil, which produce significant amounts of by-products, EVOO produced very few polar molecules and oxidative by-products. [3]

The concentration of sarcoplasmic and myofibrillar proteins in boiling pork was examined using hyperspectral imaging techniques. To enhance partial least squares regression (PLSR) models, a number of spectral pre-processing approaches were used. The best PLSR model for predicting sarcoplasmic protein amounts was constructed using seven optimum wavelengths 19 in the 400-2000 nm range without any spectral pre-processing. [4]

In their [5] study, researchers used chemometrics and hyperspectral microscope image (HMI) technology to try to replicate a human panel test for determining matcha sensory quality. The HMI system's hypercubes displayed geographic and spectral information on sample quality. Models were created using spectral data and sensory ratings from a human panel. The characteristic spectra from all of the pixels in the optimized regions of interest were then averaged. Using competitive adaptive reweighted sampling, the key spectral variables were then chosen and used to build artificial neural network models (specifically, CARS-ANN models).

V. PROPOSED METHOD

We present two analytical approaches for oil reheating in the suggested study, which adds to multispectral imaging under the food image analysis research. It's for determining the reheat level and reheat system status. It's for two reasons: one, to calculate the reheat level count class, and second, to identify major oil chemical property changes. Machine learning technique is applied for categorization of food quality condition. A novel application for MISs was provided to estimate reheat cycle count class and discrimination of substantial variations in the chemical and thermophysical parameters during repetitive heating for frying oil. For high accuracy prediction, a convolution neural network scheme-based method is used. The block diagram of the proposed method is given in Fig.1.

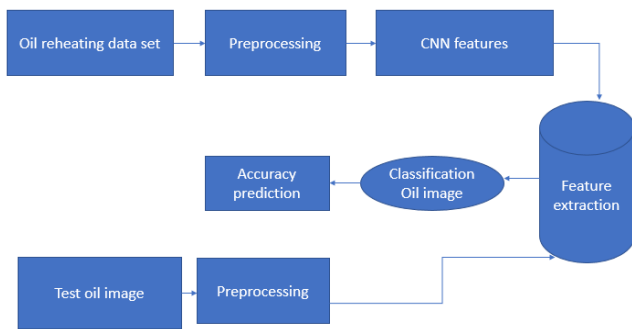


Fig. 1. Block Diagram of Proposed system

A. CNN

The structure of CNN is given in Fig.2. It is a well-known machine learning approach. One of the reasons for its popularity is that it uses automated hierarchical feature representation to recognize objects and patterns in images. CNNs make advantage of spatial links to reduce the parameters of a problem. This makes them a more practical classifier, especially in image processing, where there are several parameters (pixels), rotation, translation, and scale to consider. In actuality, CNNs avoid the drawbacks of Feed Forward Neural Networks and Multi-Layer Perceptrons by using an alternative to matrix multiplication. We apply this powerful method in this study because of the nature of OCT Image Classification using Deep Learning.

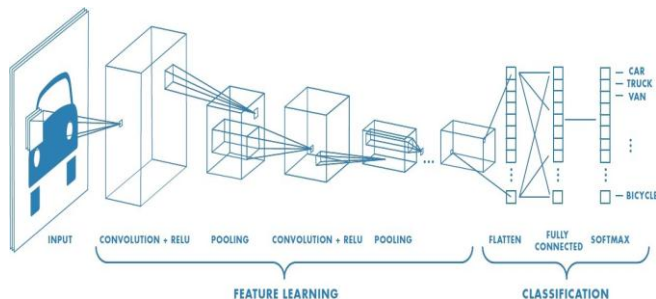


Fig. 2. CNN

Before getting into AlexNet, it's vital to understand what a convolutional neural network is. Convolutional neural networks have hidden layers that include convolutional layers, pooling layers, fully connected layers, and normalizing layers. Convolution is the technique of adding a filter to an image or signal to change it. So, what is pooling, exactly? It's a sample-based discretization approach. The main purpose is to reduce the dimensionality of the input. As a consequence, hypotheses about the properties of the binned sub-regions may be established. This is explained in further detail in Understanding Neural Networks. CNN Architecture is a multi-layer stack that converts input volume to output volume using a differentiable function. (For example, keeping track of class grades) To put it another way, a CNN

architecture is a certain arrangement of the aforementioned layers.

B. Preprocessing

Preprocessing is the process of converting raw data into a format that is more appropriate for future analysis and user comprehension. When it comes to EEG data, preprocessing entails reducing noise from the data in order to get closer to the genuine brain signals.

C. CNN Feature Extraction

Cancer Net will be the name of the network we'll create, which will be a CNN (Convolutional Neural Network). The following operations are carried out by this network: 3 CONV filters should be used. These filters should be stacked on top of each other. Max-pooling should be done. Use separable convolution by depth (more efficient, takes up less memory) It has input layers, convolution layers, ReLU layer, and maxpooling layers for extracting features from build model photos. Extraction of features The model must first be trained before it can be built.

D. Testing Process

We can split the model using a test set of 30% of the original data set because this function is implemented. D (see the code above X_train shape) is the input that simply specifies the size of the input. Instead, the main work is done in the dense layer, which takes the input and performs a linear transformation to produce an output of size one. The sigmoid activation function is the linear transformation we wish to use, resulting in a range of 0 to 1 in the output. The module Accuracy and sensitivity of the studied in this system incorporates loss per iteration, training loss, and validating loss.

VI. EXPERIMENTAL RESULTS

This dataset contains pictures from a transmittance multispectral imaging system built in-house that were used in a study to assess the quality of coconut oil.

Dataset Description

The multispectral picture generated from the imaging equipment was cropped into a 30x30 window. The clipped picture was reshaped into a 900 x 10 matrix. A pixel in the cropped picture corresponds to each row in the matrix. The first nine columns of the matrix indicate the imaging system's nine spectral bands. The label of the included class is represented in the tenth column. Each entry's value can be anything between 0 and 255.

Dataset 1:

This dataset contains photos of coconut oil that has been tainted with palm oil. There are nine stages of adulteration

in the dataset. Class 1 refers to a level of 0% adulteration. Each class increases the amount of adulteration by 5% until class9 indicates a 40% level of adulteration. There are 15 duplicates in each class. As a result, the dataset has a total of $1599900 = 121500$ rows.

Dataset2:

This dataset contains photos of coconut oil that has been tainted by warmed and reused coconut oil. There are nine stages of adulteration in the dataset. Class 1 refers to a level of 0% adulteration. Each class increases the amount of adulteration by 5% until class9 indicates a 40% level of adulteration. There are 15 duplicates in each class. As a result, the dataset has a total of $1599900 = 121500$ rows.

Dataset3:

This dataset contains photos of the coconut oil after it has been warmed and reused multiple times (days). The dataset is divided into six groups, each corresponding to a different number of days reheated, ranging from 0 to 5. There are nine duplicates in each class. As a result, the dataset has $966900 = 48600$ rows.

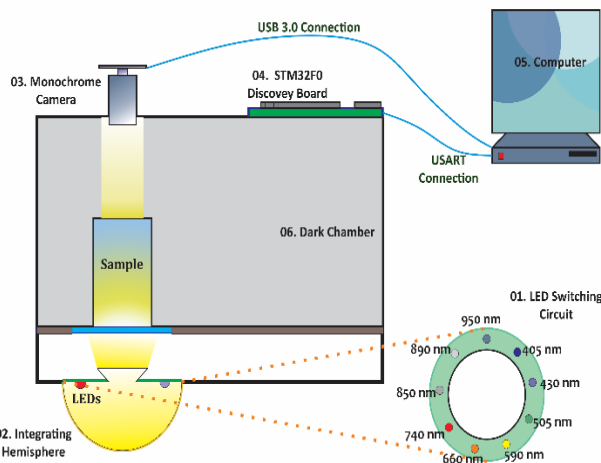


Fig. 3. Multispectral Imaging System

This multispectral imaging system was created using 9 wavelengths in the electromagnetic spectrum, ranging from ultraviolet (UV) to near-infrared (NIR). The multispectral imaging system is given in Fig.3. The system is made up of five parts, as illustrated in the diagram. A monochrome camera (FLIR Blackfly S Mono, 1.3 MP, USB3 Vision camera, resolution – 1280 x 1024, ADC – 10 bit), a monochrome camera (FLIR Blackfly S Mono, 1.3 MP, USB3 Vision camera, resolution – 1280 x 1024, ADC – 10 bit), a discovery board (STM32F0). The LED driver ICs (MAX16839ASA+) were used to control the emission intensities of all the LEDs to a near-constant level. The simulation results of the proposed system is given in Fig 4 to Fig 7.



Fig. 4. Input Image

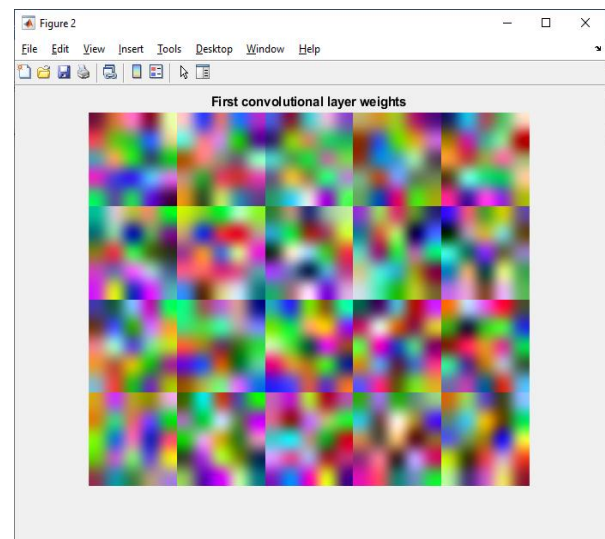


Fig. 5. Convolution layer

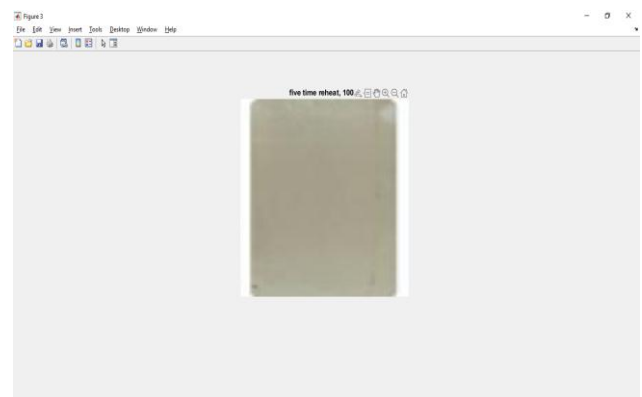
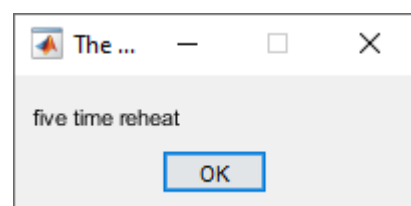


Fig. 6. Five times Reheated



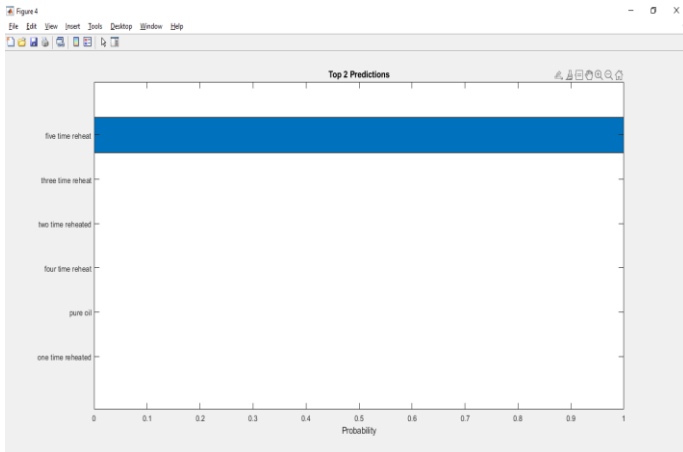


Fig. 7. Simulation result of the proposed method

VII CONCLUSION

This paper gives two novel multi-stage signal processing approaches for evaluating the level of palm oil adulteration in actual coconut oil, as well as a methodology for detecting the number of times a coconut oil sample has been cooked. The algorithms were developed for multispectral images taken from an in-house constructed transmittance-based multispectral imaging equipment. Although the classification approach showed high accuracies, the adulteration level estimation method had outstanding curve fitting ($R^2 = 0.9876$). (mode accuracy 0.90). In addition, the proposed procedures were tested on distinct samples with varying degrees of adulteration and reheating times. Even though evidenced the low mean square error 0.0029 for adulteration level determination, 0.7616 error metric for six class classification, and 0.983 error metric for qualitative classification of frequently used oil, the proposed solution could be easily modified or extended to handle a new class of adulterants and a higher number of heating cycles.

REFERENCES

[1] A. Palananda and W. Kimpan, "Turbidity of coconut oil determination using the mamoh method in image processing," *IEEE Access*, vol. 9, pp. 41 494–41 505, 2021.

[2] J. Chen, F. Liu, Z. Li, L. Tan, M. Zhang, and D. Xu, "Solid phase extraction based microfluidic chip coupled with mass spectrometry for rapid determination of aflatoxins in peanut oil," *Microchemical Journal*, vol. 167, p. 106298, 2021.

[3] D. Khamsopha, S. Woranitta, and S. Teerachaichayut, "Utilizing near infrared hyperspectral imaging for quantitatively predicting adulteration in tapioca starch," *Food Control*, vol. 123, p. 107781, 2021.

[4] Z. Saleem, M. H. Khan, M. Ahmad, A. Sohaib, H. Ayaz, and M. Mazzara, "Prediction of microbial spoilage and shelf-

life of bakery products through hyperspectral imaging," *IEEE Access*, vol. 8, pp. 176 986–176 996, 2020.

[5] H. Weerasooriya, H. Lakmal, D. Ranasinghe, W. Bandara, H. Herath, G. Godaliyadda, M. Ekanayake, and T. Madujith, "Transmittance multi spectral imaging for edible oil quality assessment," in *3D Image Acquisition and Display: Technology, Perception and Applications*. Optical Society of America, 2020, pp. JW5C–8.

[6] C.N. Nguyen, Q.T. Phan, N.T. Tran, M. Fukuzawa, P.L. Nguyen, and C.N. Nguyen, "Precise sweetness grading of mangoes (*mangifera indic.*) based on random forest technique with low-cost multispectral sensors," *IEEE Access*, vol. 8, pp. 212 371–212 382, 2020.

[7] Á. Hernández, M. T. Soria-Flrido, H. Schröder, E. Ros, X. Pintó, R. Estruch, J. Salas-Salvadó, D. Corella, F. Arós, L. Serra-Majem et al., "Role of hdl function and ldl atherogenicity on cardiovascular risk: a comprehensive examination," *PLoS One*, vol. 14, no. 6, p. e0218533, 2019.

[8] G. Prabhath, W. Bandara, D. Dissanayake, H. Hearath, G. Godaliyadda, M. Ekanayake, S. Demini, and T. Madhujith, "Multispectral imaging for detection of adulterants in turmeric powder," in *Hyperspectral Imaging and Sounding of the Environment*. Optical Society of America, 2019, pp. HTu3B–3.

[9] C. Guillaume, F. De Alzaa, and L. Ravetti, "Evaluation of chemical and physical changes in different commercial oils during heating," *Acta Scientific Nutritional Health*, vol. 2, no. 6, pp. 2–11, 2018.

[10] M. Li, M. Huang, Q. Zhu, M. Zhang, Y. Guo, and J. Qin, "Pickled and dried mustard foreign matter detection using multispectral imaging system based on single shot method," *Journal of Food Engineering*, vol. 285, p.110106, 2020.

[11] K. Lim, K. Pan, Z. Yu, and R. H. Xiao, "Pattern recognition based on machine learning identifies oil adulteration and edible oil mixtures," *Nature communications*, vol.11, no. 1, pp. 1–10, 2020

[12] S. Popa, M. S. Milea, S. Boran, S. V. Nit,u, G. E. Mos, oarca, C. Vancea, and ~ R. I. Lazau, "Rapid adulteration detection of cold pressed oils with their ~ refined versions by uv–vis spectroscopy," *Scientific reports*, vol. 10, no. 1, pp. 1–9, 2020.

[13] T. Prioleau, E. Moore, and M. Ghovanloo, "Unobtrusive and wearable systems for automatic dietary monitoring," *IEEE Transactions on Biomedical Engineering*, vol. 64, no. 9, pp. 2075–2089, 2017.

[14] R. Jamwal, S. Kumari, A. S. Dhaulaniya, B. Balan, S. Kelly, A. Cannavan, D. K. Singh et al., "Utilizing atr-ftir spectroscopy combined with multivariate chemometric

modelling for the swift detection of mustard oil adulteration in virgin coconut oil," *Vibrational Spectroscopy*, vol. 109, p.103066, 2020.

[15] V. B. Raju and E. Sazonov, "Detection of oil-containing dressing on salad leaves using multispectral imaging," *IEEE Access*, vol. 8, pp. 86 196– 86 206, 2020.